

CONDENSED-MATTER  
SPECTROSCOPY

## Fluorescence of the Nematic Liquid Crystal 5CB in Nanoporous Glasses

O. V. Yaroshchuk<sup>a</sup>, Yu. P. Piryatinskiĭ<sup>a</sup>, L. A. Dolgov<sup>a</sup>, T. V. Bidna<sup>a</sup>, and D. Enke<sup>b</sup>

<sup>a</sup> Institute of Physics, National Academy of Sciences of Ukraine, Kiev, 03028 Ukraine

<sup>b</sup> Institute of Technical and Macromolecular Chemistry, Martin Luther University, Halle, D-06108 Germany

Received February 22, 2005

**Abstract**—The fluorescence spectra of the nematic liquid crystal *n*-pentyl-*n*'-cyanobiphenyl (5CB) in porous glasses with pores from 1 to 44 nm in diameter are investigated. A decrease in the pore diameter leads to suppression of some long-wavelength spectral components corresponding to *H*-type predimer and dimer pairs (the molecular sieve effect). The spectrum of 5CB in small pores (smaller than 4 nm in diameter) can be explained by the superposition of the monomer fluorescence and the fluorescence of *J*-type dimer pairs of 5CB molecules, as well as associates of 5CB molecules and surface groups on pore walls. Exposure of samples to UV light enhances the molecular interaction in associates, possibly, due to the formation of strong chemical bonds.

PACS numbers: 33.50, 42.70

DOI: 10.1134/S0030400X06030143

### INTRODUCTION

Liquid crystals (LCs) are characterized by the presence of phases that are intermediate (mesophases) between the crystalline and liquid phases. Such mesophases combine the properties of liquid and crystalline phases, in particular, fluidity and anisotropy. The mesomorphic state is characteristic of macro- and microvolumes of LCs, up to sizes of several hundredths of a micrometer. With a decrease in the size of the LC phase to several nanometers, the transition from the nematic mesophase to an isotropic liquid blurs, while some smectic mesophases are completely suppressed [1, 2]. This effect indicates the presence of a size limit below which the realization of LC mesophases is thermodynamically unfavorable. The existence of this limit is due, in particular, to spatial limitations (specifically, the strong dispersivity of LCs, which does not allow for collective self-ordering effects). It can be easily estimated that the thermodynamic size limit is reached when the surface and volume fractions of LC molecules in a nanovolume become comparable. In this context, a significant interphase interaction (in particular, physical and chemical adsorption of LC molecules on walls) is another important factor of suppression of the mesomorphic state of LCs in nanopores. Analysis of the competition between the intraphase and interphase interactions and their effect on the characteristics of LC volumes is an interesting scientific problem. Study of this competition may lead to the discovery of new transition effects, quantum-mechanical phenomena, and unusual physical properties of small LC volumes.

The purpose of our investigation was to gain insight into the fluorescence of LC molecules in nanoporous matrices. The dependence of the fluorescence spectra

on the pore size was investigated and the fluorescence characteristics of micro- and nanovolumes were compared. Previously, we investigated a nematic azoxy compound with pronounced photochemical properties [3]. It was shown that incorporation of this LC into nanopores radically changes its fluorescence spectrum and photochemical properties.

In this study, we used a more photochemically stable nematic: *n*-pentyl-*n*'-cyanobiphenyl (5CB), which has a high fluorescence quantum yield. The fluorescence properties of macroscopic volumes of 5CB in the LC, crystalline, and isotropic states have been intensively studied by several research groups [4–8]. We have also carried out such investigations during the last few years [9, 10]. These investigations [4–10] showed that the complex structure of the fluorescence spectrum of 5CB can be explained by the combination of the fluorescence of monomers, dimers, and excimers. Note that the excimer fluorescence is determined by several types of predimer states characterized by different stereochemistry and interaction of molecules. According to the results of the present study, some long-wavelength persistent components of the spectra of 5CB in nanopores are suppressed, which indicates that the formation of some types of molecular associates is hindered. This phenomenon is related to steric hindrances and the pore surface effect. We also studied the effect of UV irradiation on the fluorescence spectrum of 5CB in nanopores.

### EXPERIMENTAL

#### *Objects of Study*

As porous matrices, we used porous glasses with different pore sizes prepared at the Institute of Techni-

cal and Macromolecular Chemistry of Martin Luther University (Halle, Germany). Porous glasses were fabricated from initial sodium borosilicate glasses using the technique described in [11]. A spongelike structure with through pores was formed by leaching and removal of the sodium borosilicate phase. As a result, a framework composed mainly of  $\text{SiO}_2$  remained. The porosity and the average pore diameter could be specified by varying the leaching conditions. Plates 0.5 mm thick were cut from a thus-processed glass sample and subjected to grinding.

The porous glasses were characterized by the nitrogen absorption method [11]. These investigations showed, in particular, that the distribution of nanopore diameters is rather narrow, which is indicative of a fairly high degree of monodispersity. The average pore diameter  $d$  in the samples studied was 1, 4, 14, and 44 nm. The porosity of glasses varied from 21% ( $d = 1$  nm) to 39% ( $d = 14$  nm). Before filling with an LC, porous plates were immersed in toluene for several hours and then annealed at  $450^\circ\text{C}$  for 2 h.

As the LC filler, we used 5CB (Merck Corporation). This material has a nematic phase in the temperature range  $18$ – $35^\circ\text{C}$ . At temperatures below  $18^\circ\text{C}$ , 5CB is crystallized. Above  $35^\circ\text{C}$ , it passes to the isotropic state. The filling of porous matrices with the LC was carried out by immersing porous plates in an LC melt ( $T = 80^\circ\text{C}$ ) and soaking the plates in the melt for 3 h. After extraction, the surface of the porous plates was carefully wiped to eliminate the LC residue.

### Experimental Methods

The main experimental method was fluorescent spectroscopy (see [9] for details). Steady-state and time-resolved fluorescence spectra were recorded using an MDR-12 monochromator (LOMO, Russia) with a photoadapter and stored in a computer. During the measurements, the spectrometer slit width was  $0.2$ – $0.4$  nm. Fluorescence was excited by a pulsed nitrogen laser at a wavelength  $\lambda = 337.1$  nm with a pulse width of 9 ns, a pulse repetition frequency of 100 Hz, and a pulse power of 5 kW. To measure time-resolved fluorescence spectra and the fluorescence kinetics at different wavelengths, we used a sampling system with a time window of 0.1 ns. This system made it possible to record fluorescence spectra with different time delays  $t_d$  with respect to the laser pulse. The time resolution of the system was no worse than 0.7 ns. In measurements of the fluorescence spectra, the time resolution was determined by the steepness of the leading edge of the laser pulse. In fluorescence kinetic measurements, this characteristic was determined by the oscilloscope strobe width (0.1 ns).

The fluorescence spectra were investigated at 298 and 77 K. To avoid a photochemical effect due to the action of a laser pulse on the LC during the fluorescence measurements, the laser beam was defocused

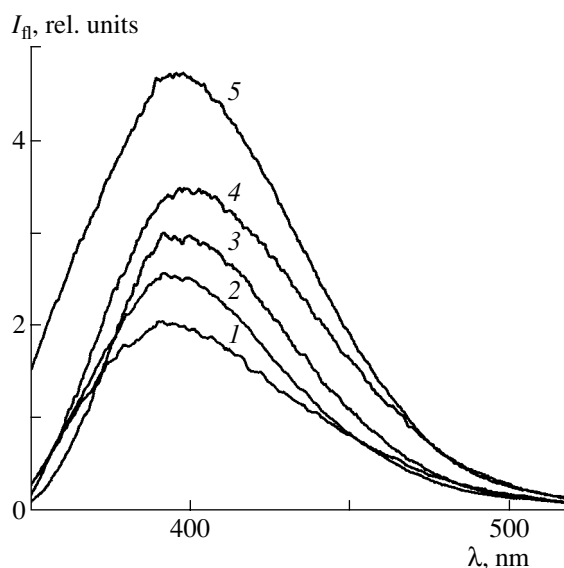


**Fig. 1.** Steady-state fluorescence spectra of 5CB in (1–4) porous glasses with pore diameters of (1) 1, (2) 4, (3) 14, and (4) 44 nm and (5) a 5- $\mu\text{m}$ -thick layer, measured at 298 K.

near the sample into a spot 8 mm in diameter. For the same reason, the samples were not subjected to long-term UV irradiation. The specific features of the fluorescence of UV-irradiated samples were studied separately. A high-pressure DRSh-500 mercury lamp was used as a UV source. Both the entire radiation spectrum (white light) and its component at  $\lambda = 365$  nm, selected by an interference filter, were used. The radiation intensity in these cases was, respectively, 100 and  $6 \text{ mW/cm}^2$ . The irradiation time was always 30 min. The time interval between the UV irradiation and spectral measurements was 5–15 min.

### RESULTS

As was noted previously in [3], the porous glasses we used fluoresce under UV irradiation and their fluorescence spectrum depends strongly on the pore size. However, the fluorescence quantum yield of porous glasses is more than an order of magnitude lower than the fluorescence quantum yield of 5CB. Therefore, we neglect below the fluorescence of porous glasses.

Figure 1 shows the steady-state fluorescence spectra of 5CB in nanopores with sizes of 1, 4, 14, and 44 nm. For comparison, the fluorescence spectrum of a 5CB layer with a thickness  $d = 5 \mu\text{m}$  placed between two quartz plates is also shown. It can be seen that, with decreasing pore diameter, the fluorescence peak shifts to shorter wavelengths: from 400 nm at  $d = 44$  nm to 390 nm at  $d = 1$  nm. Simultaneously, the fluorescence intensity decreases. Obviously, this phenomenon is related to the decrease in the glass porosity.

To eliminate noises, the lifetimes were measured at wavelengths of 380 and 420 nm, which differ signifi-

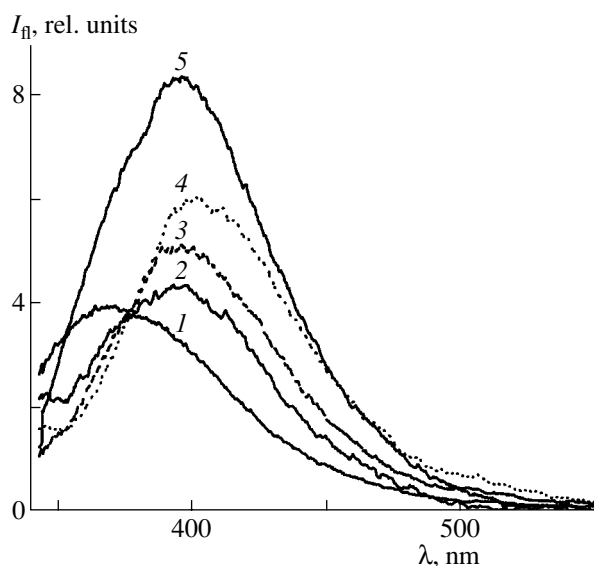


**Fig. 2.** Time-resolved fluorescence spectra of 5CB in (1–4) porous glasses with pore diameters of (1) 1, (2) 4, (3) 14, and (4) 44 nm and (5) a 5- $\mu\text{m}$ -thick layer, measured at 298 K with a time delay  $t_d = 0\text{--}0.7$  ns after the onset of excitation.

cantly from the excitation wavelength of 337.1 nm. The probe wavelength  $\lambda_{fl} = 380$  nm corresponds to the overlap of the fluorescence bands of monomers and dimer associates of 5CB molecules. In turn, the value  $\lambda_{fl} = 420$  nm corresponds to the excimer fluorescence [9]. At  $\lambda_{fl} = 380$  nm, in the spectra of a thick LC layer ( $d = 5$   $\mu\text{m}$ ) and (somewhat less clearly) the LC in pores with the diameter  $d = 44$  nm, two fluorescence components can be selected with the lifetimes  $\tau_1 = 5.9$  ns and  $\tau_2 = 10.3$  ns. In the spectra of 5CB in nanopores with the diameter  $d \leq 14$  nm, one component is dominant. Its characteristic time depends on the pore size: 6.1, 4.2, and 3.0 ns for pore diameters of 14, 4, and 1 nm, respectively. Similarly, at  $\lambda_{fl} = 420$  nm, two fluorescence components with  $\tau_1 = 8.8$  ns and  $\tau_2 = 22$  ns can be selected in the spectrum of the LC in pores with  $d = 44$  nm, while there is only one component for 5CB in nanopores of smaller diameter. For nanopores with diameters of 14, 4, and 1 nm, the characteristic times are, respectively, 8.5, 4.4, and 4.1 ns. Two conclusions can be drawn on the basis of these data. First, in comparison with the microscale layer, the component with  $\tau_2 = 22$  ns is almost absent in the spectra of the LC in nanopores with  $d \leq 14$  nm. This fact was explained previously by the excimer fluorescence [9, 10]. Second, the fluorescence time in nanopores decreases with decreasing pore size.

The largest difference is observed for the fluorescence spectra measured at the initial instant of time ( $t_d = 0\text{--}0.7$  ns) after the pulsed laser excitation. Figure 2 shows the time-resolved fluorescence spectra of 5CB in nanopores 1, 4, 14, and 44 nm in diameter, as well as the spectrum of a 5- $\mu\text{m}$ -thick 5CB layer. One can see a

tendency of the fluorescence spectrum to hypsochromic shift with decreasing pore size. Analysis of the fluorescence spectra measured with short and long time delays  $t_d$  (Figs. 2 and 1, respectively) shows that two bands at 380 and 395 nm can be selected in the spectrum of the 5CB layer and two bands at 370 and 395 nm are present in the spectrum of the LC in nanopores with  $d > 1$  nm. With a decrease in the pore size, the intensity of the band at 395 nm decreases, while that of the band at 370 nm increases.

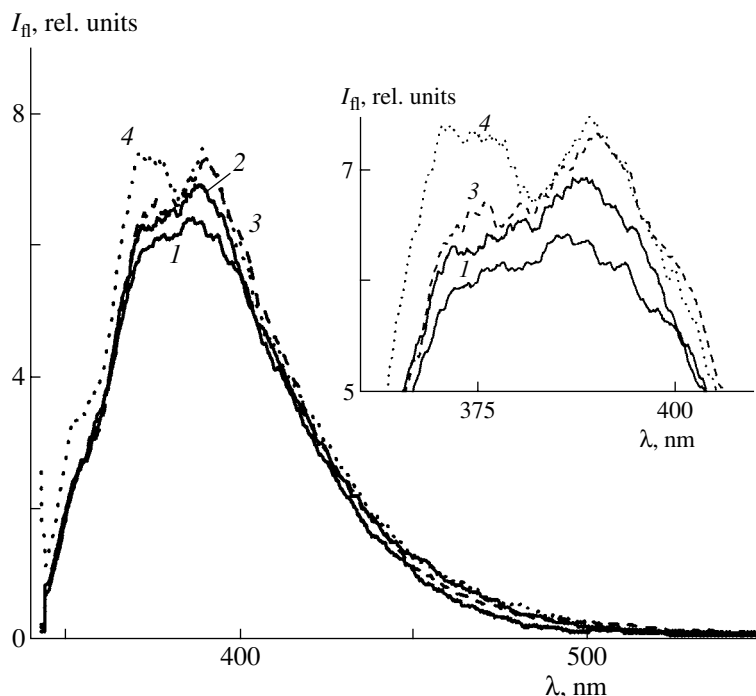
The low-temperature fluorescence spectra of 5CB ( $T = 77$  K) in pores of different diameter are shown in Fig. 3. At  $d > 1$  nm, the structure of the spectrum manifests itself in the form of bands at 372 and 390 nm. The spectrum of the 5CB in pores with  $d = 1$  nm, as at 298 K, contains a structureless band at 386 nm with a shoulder at about 355 nm.

Figure 4 shows the steady-state fluorescence spectra of 5CB in a microvolume and in nanoporous glasses after irradiation by a mercury lamp (the entire radiation spectrum). Ultraviolet irradiation leads to a bathochromic shift of the spectra of all samples and an increase in the fluorescence quantum yield by a factor of about 3. It can be seen from Fig. 4 that the red shift of the fluorescence peak is the largest for the irradiated 5CB in a macroscopic volume and in large pores. In the latter case, the fluorescence peak corresponds to a wavelength of 410 nm, whereas, for the LC in the smallest pores ( $d = 1$  nm), the corresponding wavelength is 405 nm.

The effect of UV irradiation is more pronounced in the time-resolved fluorescence spectra. The spectra shown in Fig. 5 indicate that, at the delay time  $t_d = 0.7$  ns, the fluorescence peaks are located at longer wavelengths than at  $t_d = 5$  ns. Thus, in contrast to the fluorescence spectra of the unirradiated samples, the lifetimes of the long-wavelength spectral components are shorter than those of the short-wavelength components.

Investigation of the fluorescence kinetics of the irradiated samples showed that the fluorescence decay is described well by two characteristic times. The shorter time  $\tau_1$  dominates in the long-wavelength spectral region ( $\lambda_{fl} > 410$  nm) and the longer time  $\tau_2$  is dominant at shorter wavelengths. With a decrease in the pore diameter, the lifetimes  $\tau_1$  and  $\tau_2$  decrease and become closer to each other. For example, for the irradiated layer with a thickness of 5  $\mu\text{m}$  and porous samples with pore diameters of 44, 14, 4, and 1 nm, the lifetime  $\tau_1$  is 6, 5.9, 4.2, and 4.2 ns and  $\tau_2$  is 13.4, 6.4, 4.2, and 4.2 ns, respectively. Therefore, at pore diameters smaller than 4 nm, the fluorescence relaxation kinetics in irradiated samples is determined mainly by one lifetime.

It can also be seen from Fig. 5 that, with a decrease in the diameter of nanopores, the fluorescence peaks become closer to each other at both delay times. For example, for the samples with pore diameters of 14, 4, and 1 nm, the fluorescence peaks are located, respec-



**Fig. 3.** Time-resolved fluorescence spectra of 5CB in porous glasses with pore diameters of (1) 1, (2) 4, (3) 14, and (4) 44 nm, measured at 77 K with a time delay  $t_d = 0-0.7$  ns after the onset of excitation. The bands at 372 and 390 nm are shown in detail in the inset.

tively, at 414, 412, and 409 nm at  $t_d = 0.7$  ns and at 404, 410, and 412 nm at  $t_d = 5$  ns. This result, along with the decrease in the difference in the characteristic relaxation times, indicates that the fluorescence in the irradiated samples with  $d \leq 4$  nm is described mainly by one type of emitters.

To conclude, we should note that all regularities of the fluorescence of the samples exposed to white light of a mercury lamp are also valid for the samples subjected to monochromatic ( $\lambda = 365$  nm) irradiation. This fact indicates the determining role of the same types of photochemical transformations in both cases of irradiation.

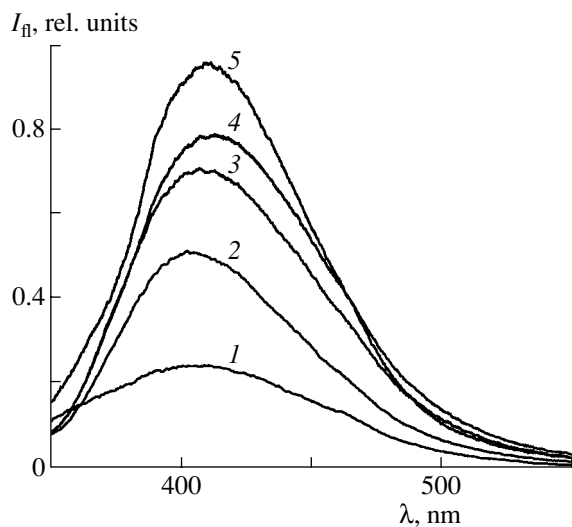


**Fig. 4.** Steady-state fluorescence spectra of UV-irradiated 5CB in (1-4) porous glasses with pore diameters of (1) 1, (2) 4, (3) 14, and (4) 44 nm and (5) a 5- $\mu\text{m}$ -thick layer, measured at 297 K. The samples were exposed to white light of a mercury lamp ( $100 \text{ mW/cm}^2$ , 30 min).

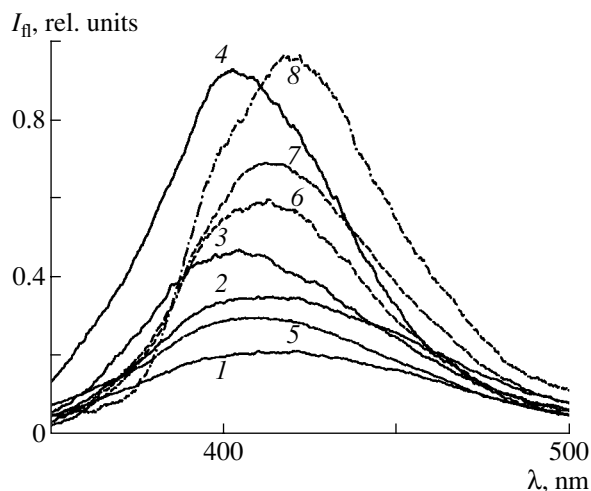


**Fig. 5.** Time-resolved fluorescence spectra of UV-exposed 5CB in (1-3, 5-7) porous glasses with pore diameters of (1, 5) 1, (2, 6) 4, and (3, 7) 14 nm and (4, 8) a 5- $\mu\text{m}$ -thick layer, measured at 297 K with time delays  $t_d = (5-8) 0.7$  and (1-4) 5 ns. The samples were exposed to white light of a mercury lamp ( $100 \text{ mW/cm}^2$ , 30 min).

tion. The most probable transformations are discussed in the next section.

## DISCUSSION

Before proceeding to the interpretation of the spectra of 5CB in nanopores, let us briefly summarize the specific features of the fluorescence of 5CB in a macroscopic volume, which was studied previously [4–10]. In the spectra of strongly diluted molecular solutions of 5CB, a band at  $\lambda_{fl} = 330\text{--}340$  nm is observed, which is due to the fluorescence of monomer molecules. In concentrated solutions, this band manifests itself only as a shoulder. At the same time, a wide band peaked at  $\lambda_{fl} = 380\text{--}400$  nm arises, which is due to the fluorescence of molecular associates, primarily excimers [6].

The fluorescence spectrum of the 5CB layer is similar to the spectrum of a concentrated solution. It can be arbitrarily divided into short-wavelength ( $\lambda_{fl} = 320\text{--}380$  nm) and long-wavelength ( $\lambda_{fl} = 380\text{--}500$  nm) ranges. In the range from 320 to 380 nm, a band polarized along the long axis of LC molecules, which is due to the monomer emission from the  ${}^1L_a$  state, can be selected [12]. This band corresponds to the band at 280 nm in the absorption and fluorescence excitation spectra. The long-wavelength range in the fluorescence spectrum ( $\lambda = 380\text{--}500$  nm) has a complex structure. As we showed previously in [9], bands at 380, 395, and 405 nm can be selected in this range, which correspond to different associates of 5CB molecules.

Fluorescence with a large lifetime ( $\tau = 22$  ns) in the band at 405 nm is characteristic of classical excimers. The corresponding predimer pairs are generally formed from noncoplanar 5CB molecules by sandwich packing. Due to the steric hindrances, molecules are located at a relatively large distance from each other in such pairs. In the excited state, such molecules are flattened [7]. As a result, the interaction in pairs is enhanced and excimers are formed. At low temperatures ( $T < 77$  K), the band at 405 nm is not observed, which also indicates the excimer nature of the fluorescence [9].

The fluorescence bands at 380 and 395 nm are observed at both room and low temperatures. The latter circumstance indicates that this fluorescence is not of activation type and is not related to excimers. It is suggested that these bands correspond to molecular pairs with much stronger bonds than those in predimer pairs, which generate excimers upon photoexcitation. Apparently, such pairs are physical dimers, which were described well in studies devoted to the 5CB LC [13]. In the excitation spectra, the bands at 270 and 294 nm (red- and blue-shifted with respect to the monomer absorption band at 280 nm) correspond to the fluorescence bands at 380 and 395 nm, respectively. This circumstance gives grounds to suggest that dimers are formed in a macroscopic volume of 5CB through both the *H* and *J* aggregation mechanisms (with sandwich and linear packings, respectively). Certainly, we speak

about the preferred type of packing since there are many intermediate types, characterized by different degrees of electronic overlap. Within this suggestion, the fluorescence band at 395 nm is due to *J* dimers. The band at 380 nm may be due to *H* dimers if emission occurs from a partially relaxed state. As is known, it is difficult to observe direct fluorescence of *H* aggregates because of the high energy of their excited level and, therefore, the high probability of their transition to lower levels with subsequent emission. *H* dimers can be formed only by highly coplanar conformers, which can closely approach each other. Thus, the presence of several fluorescence bands in the long-wavelength spectral range can be easily explained by the existence of different molecular associates (predimer and dimer pairs) of *H* and *J* types, formed by molecules with different stereochemistry and degrees of bonding.

Previously, we also investigated the fluorescence spectrum of a layer of 5CB molecules deposited on a quartz substrate [9]. In this spectrum, a band at 370 nm and a shoulder at 340 nm manifest themselves. The shoulder at 340 nm is due to the monomer fluorescence, while the band at 370 nm is due to the fluorescence of both monomers and surface molecular associates with fairly strong bonds (complexes of 5CB molecules with surface groups of the quartz substrate and, possibly, 5CB dimers of a certain type that is not characteristic of a macroscopic volume).

As was noted above, in the fluorescence spectra of 5CB in pores with  $d \leq 14$  nm, the band at 405 nm with a lifetime of 22 ns, which is responsible for the excimer fluorescence of macroscopic volumes of 5CB, is almost absent. Therefore, the formation of *H* predimer pairs yielding excimer fluorescence is hindered in such nanopores. The absence of a pronounced band at 380 nm in the spectra of 5CB in nanopores confirms that the formation of *H* dimers is hindered. At the same time, the band at 395 nm remains in the spectra with a decrease in the pore size to  $d = 1$  nm, which is indicative of the absence of significant hindrances to the formation of *J* dimers. According to Fig. 2, on transition from  $d = 4$  nm to  $d = 1$  nm, even more radical changes occur in the fluorescence spectrum: the short-lived component peaked at 370 nm detected previously for a molecular 5CB layer sharply increases. Such behavior is also observed for the fluorescence lifetimes (at  $\lambda_{fl} = 380$  nm,  $\tau$  is 1.5 and 3 ns for the molecular 5CB layer and 5CB in the pores with  $d = 1$  nm, respectively). Therefore, as in the case of the molecular layer, the band at 370 nm can be due to the strong effect of the surface, facilitating an increase in the monomer fraction and the formation of surface associates.

Thus, the penetration of *H* dimers and predimers into nanopores (or their formation in these nanopores) is significantly hindered. It follows from the above considerations that such states are significantly suppressed due to the interaction of 5CB molecules with the substrate. This observation is in good agreement with the

results of other researchers, who confirmed the dissociation of 5CB dimers at the LC/substrate interface [14, 15]. In addition, the steric factor should be taken into account. The spatial limitations in nanopores also hinder molecular aggregation (primarily, *H* aggregation) [16]. Indeed, the transverse size of a 5CB molecule (0.3 nm) is comparable with the pore diameter. Single molecules can penetrate such pores, but the incorporation of *H* associates is hindered. At the same time, the steric factor allows for *J* aggregation, which is characterized by linear arrangement of molecules along a pore. In fact, nanoporous glass acts as a molecular sieve, rejecting *H* associates.

The bathochromic shift of the fluorescence spectrum of UV-irradiated porous glass filled with 5CB, as in the macroscopic case [10], indicates the increasing contribution of the fluorescence of molecular associates. The decrease in the fluorescence lifetime in the long-wavelength spectral region can be explained by the enhancement of the interaction in molecular pairs, in particular, due to the formation of chemical bonds. If we take into account that the most likely process for the unirradiated samples is the formation of 5CB associates of the *J* type, as well as associates of 5CB molecules with surface molecular groups of the pore walls, the linear photopolymerization of 5CB molecules and the formation of stable complexes of 5CB molecules with the pore surface seems to be quite likely. Based on the tendency of the fast and slow spectral components to approach each other with a decrease in the pore diameter (Fig. 5), we can suggest that one of the mechanisms proposed or a combination of them is dominant in narrow pores. We hope to solve this problem by the end of our IR studies.

## CONCLUSIONS

Thus, some components characteristic of a macroscopic volume are suppressed in the fluorescence spectra of LC 5CB in nanoporous glasses. In particular, the excimer fluorescence band at 410 nm, as well as the band at 380 nm, which is due to dimers, is not observed in the spectra of these materials. In addition, at  $d \leq 1$  nm, the short-wavelength spectral component ( $\lambda_{fl} = 370$  nm) sharply increases, which is indicative of the increasing role of the monomer fluorescence and the formation of surface associates. Such transformations of the fluorescence spectrum indicate that the formation of dimers and predimers of the *H* type is significantly hindered. The reasons for this phenomenon are the interaction of 5CB molecules with the substrate and spatial limitations. Based on only the fluorescence data, it is difficult to determine which of these factors plays the key role. Although we observed rejection of molecular *H* associates by narrow pores, we did not observe

any significant difficulties in the formation of *J* associates of 5CB molecules. In addition, the formation of surface associates is likely, primarily, complexes of 5CB molecules with surface fragments of pore walls (for example, with bonding similar to hydrogen bonding [17]). The fluorescence spectra of UV-irradiated samples show that the intermolecular bonding in such associates can be enhanced upon UV irradiation; in particular, strong chemical bonds can be formed.

## ACKNOWLEDGMENTS

This study was supported by the targeted projects VTs 89 and VTs 89-297-13 of the National Academy of Sciences of Ukraine.

## REFERENCES

1. G. S. Iannacchione, S. H. Qian, G. P. Crawford, et al., *Mol. Cryst. Liq. Cryst.* **262**, 13 (1995).
2. G. S. Iannacchione, G. P. Crawford, S. Žümmer, et al., *Phys. Rev. Lett.* **71** (16), 2595 (1993).
3. Yu. P. Piryatinskiĭ, O. V. Yaroshchuk, L. O. Dolgov, et al., *Opt. Spektrosk.* **97** (4), 566 (2004) [*Opt. Spectrosc.* **97** (4), 537 (2004)].
4. V. V. Danilov, Yu. T. Mazurenko, and D. A. Savel'ev, *Opt. Spektrosk.* **57**, 748 (1984) [*Opt. Spectrosc.* **57**, 455 (1984)].
5. V. V. Danilov, L. P. Zagaĭnova, G. V. Klimusheva, et al., *Khim. Fiz.* **8** (2), 214 (1989).
6. T. Ikeda, S. Kurihara, and S. Tazuke, *J. Phys. Chem.* **94** (17), 6550 (1990).
7. J. I. Kukielski, *J. Mol. Struct.* **478**, 1 (1999).
8. S. Kato, B. Lee, and C. Pac, *Liq. Cryst.* **22** (5), 595 (1997).
9. Yu. P. Piryatinskiĭ and O. V. Yaroshchuk, *Opt. Spektrosk.* **89** (6), 937 (2000) [*Opt. Spectrosc.* **89** (6), 860 (2000)].
10. Yu. P. Piryatinskiĭ and O. V. Yaroshchuk, *Opt. Spektrosk.* **92** (4), 569 (2002) [*Opt. Spectrosc.* **92** (4), 517 (2002)].
11. S. P. Zhdanov, in *Physics and Chemistry of Silica Dioxides*, Ed. by M. M. Shul'ts and R. G. Grebenshchikov (Nauka, Moscow, 1987) [in Russian].
12. C. David and D. Baeyens-Volant, *Mol. Cryst. Liq. Cryst.* **59**, 18 (1980).
13. J. E. Lydon and C. J. Coacley, *J. Phys., Colloq.* **36**, 45 (1975).
14. M. Oh-e, S.-C. Hong, and Y. R. Shen, *J. Phys. Chem. B* **104**, 7455 (2000).
15. T. Sakai, K. Shirota, T. Yamada, et al., *Jpn. J. Appl. Phys.* **35**, 3971 (1996).
16. M. Kasha, H. R. Rawls, and M. A. Boyoumi, *Pure Appl. Chem.* **11**, 371 (1965).
17. I. Gnatyk, G. Puchkowska, O. Yaroshchuk, et al., *J. Mol. Struct.* **555**, 235 (2000).

*Translated by Yu. Sin'kov*